Light charged particle multiplicities in fusion and quasifission reactions

Sh.A. Kalandarov, G.G. Adamian, N.V. Antonenko,
D. Lacroix, J.P. Wieleczko

BLTP, JINR
IPN Orsay
GANIL

Content

- ***Introduction***
- ***Model***
- ***Results & Discussion***
- ***Summary***

Introduction

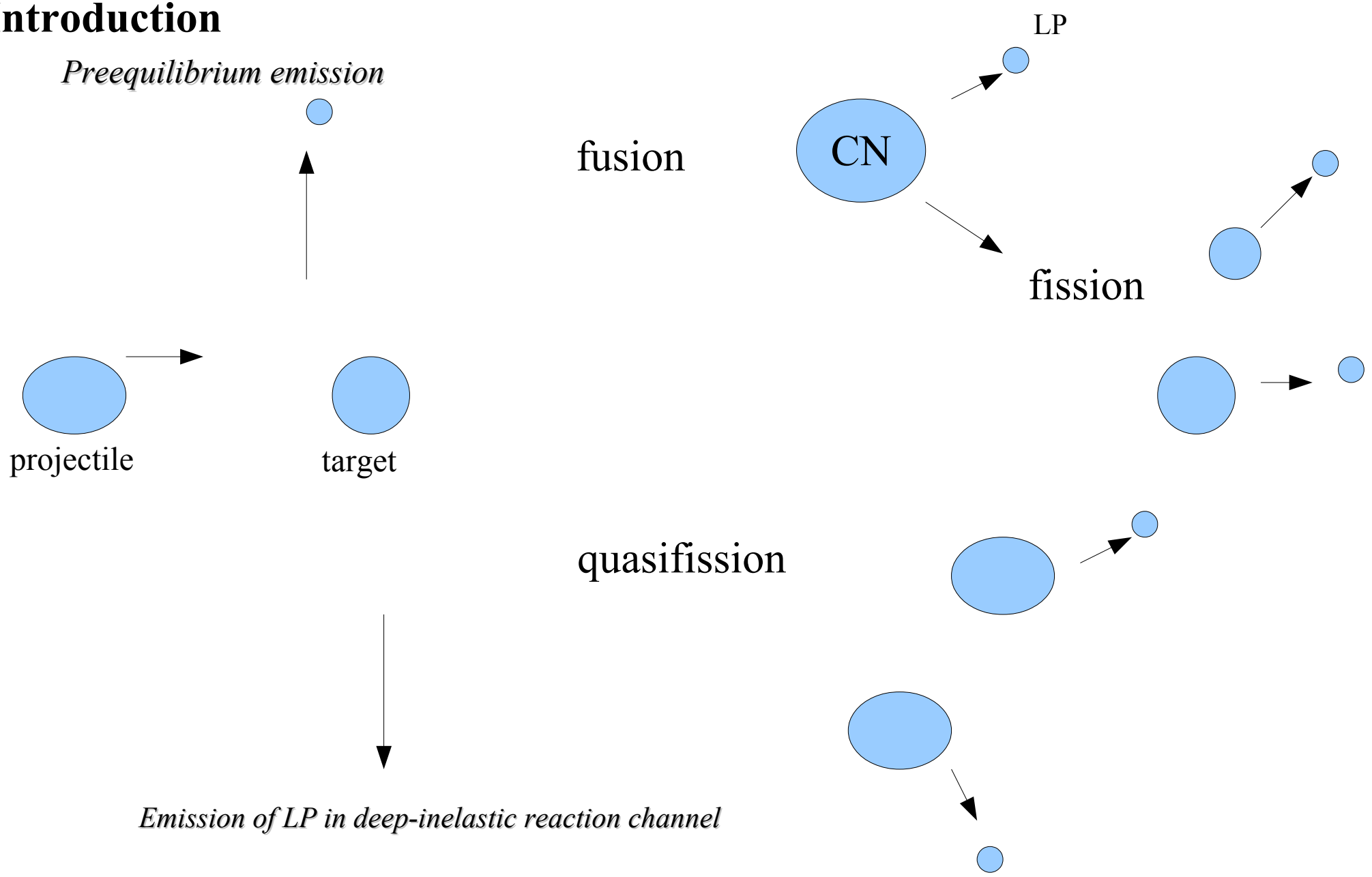

Model

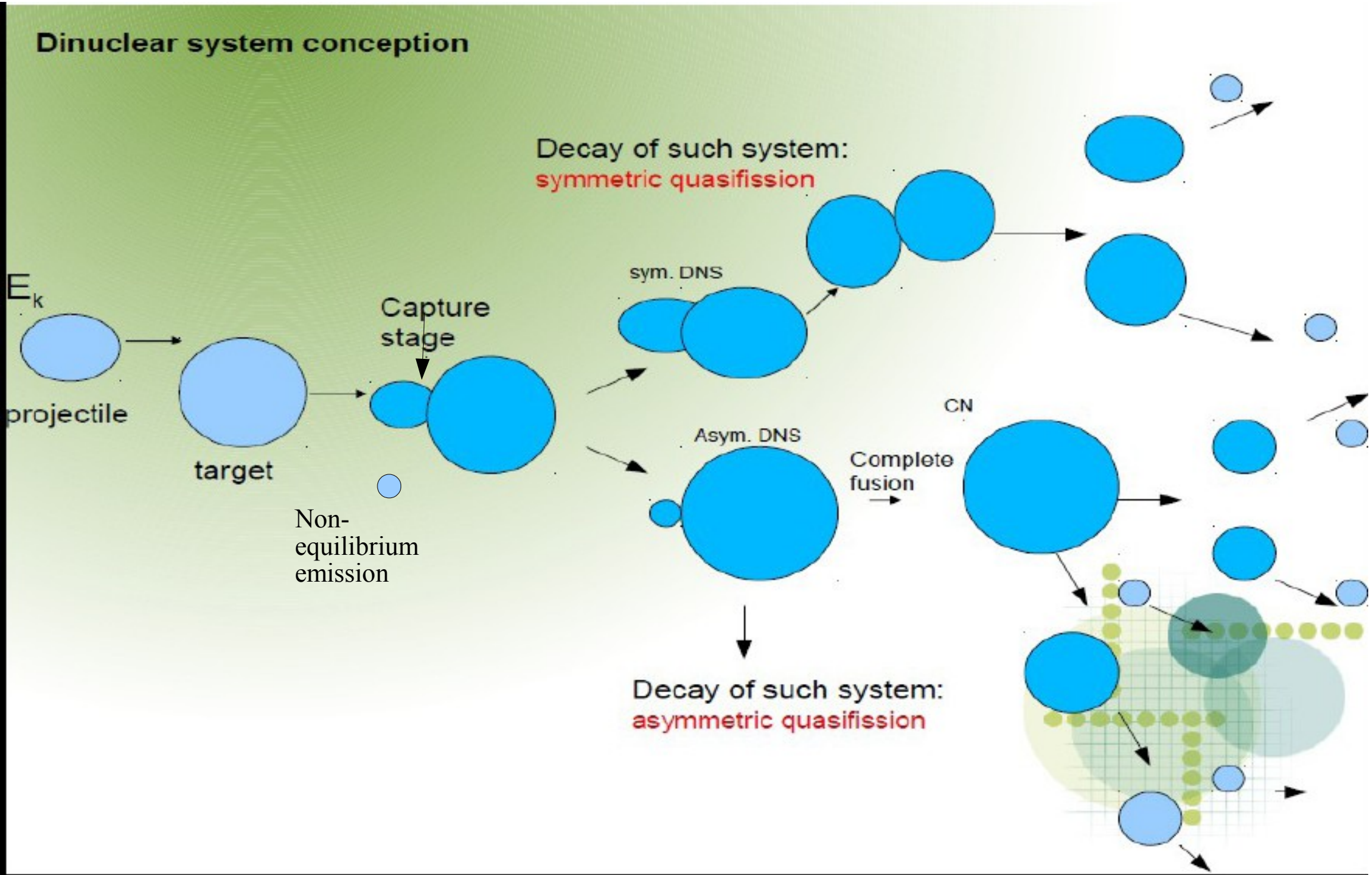
Dinuclear system conception
Decay of such system:
symmetric quasifission
E_k
projectile
target
Capture
stage
sym. DNS
Asym. DNS
CN
Complete
fusion
Non-
equilibrium
emission
Decay of such system:
asymmetric quasifission

The production cross section of the residual nucleus with certain mass number A and charge number Z is given as

$$\sigma_{Z,A}(E_{\mathrm{c.m.}}) = \sum_{J=0}^{J_{max}} \sigma_{Z,A}(E_{\mathrm{c.m.}}, J)$$

$$= \sum_{J=0}^{J_{max}} \sigma_{\mathrm{cap}}(E_{\mathrm{c.m.}}, J) W_{Z,A}^{sur}(E_{\mathrm{c.m.}}, J),$$

where σ_{cap} is the partial capture cross section which defines the transition of the colliding nuclei over the Coulomb barrier and the formation of the initial DNS when the kinetic energy $E_{\mathrm{c.m.}}$ and angular momentum J of the relative motion are transformed into the excitation energy and angular momentum of the DNS. The probability of the production of certain residual nucleus (Z, A) from the excited entrance channel DNS in a distinct decay channel is described by $W_{Z,A}^{sur}(E_{\mathrm{c.m.}}, J)$.

Capture

$$\sigma_{\rm cap}(E_{\rm c.m.},J) = \pi\lambda\!\!\!^{-2}(2J+1)P_{\rm cap}(E_{\rm c.m.},J),$$

where $\lambda\!\!\!^{-2} = \hbar^2/(2\mu E_{\rm c.m.})$ is the reduced de Broglie wavelength and μ the reduced mass in the entrance channel. The transition probability is calculated with the Hill-Wheeler formula: $P_{\rm cap}(E_{\rm c.m.},J) = (1+\exp[2\pi(V(R_b,J)-E_{\rm c.m.})/\hbar\omega(J)])^{-1}$, where the effective nucleus-nucleus potential V is approximated near the Coulomb barrier at $R = R_b$ by the inverted harmonic-oscillator potential with the barrier height $V(R_b,J)$ and frequency $\omega(J)$

The maximum value of the angular momentum J_{max} is limited either by the kinematic angular momentum $J^{kin}_{max} = [2\mu(E_{\rm c.m.} - V(R_b,0))]^{1/2}R_b$ or by the critical angular momentum J_{cr} depending on which one is smaller: $J_{max} = \min\{J^{kin}_{max}, J_{cr}\}$.

To calculate $W^{sur}_{Z,A}(E_{\rm c.m.}, J)$, one has to find the formation-emission probability $W_{Z_1,A_1}(E_{\rm c.m.}, J)$ of a certain light particle or cluster (Z_1, A_1) from the excited entrance channel DNS. Here, we consider the decay of the excited nuclear system as a sequential light particle ($Z_1 < 2$) evaporation, which includes neutrons, protons, deutrons, and tritons, and complex clusters ($Z_1 \geq 2$). The $W_{Z_1,A_1}(E_{\rm c.m.}, J)$ is calculated as the product of the CN or DNS formation probability P_{Z_1,A_1} and the CN or DNS decay probability $P^R_{Z_1,A_1}$

$$W_{Z_1,A_1}(E_{\rm c.m.}, J) = \frac{P_{Z_1,A_1} P^R_{Z_1,A_1}}{\sum_{Z'_1,A'_1} P_{Z'_1,A'_1} P^R_{Z'_1,A'_1}},$$

where the indexes Z'_1 and A'_1 go over all possible channels from the neutron evaporation to the symmetric splitting.

The probability of the CN or DNS formation

$$P_{Z_1,A_1}(E_{\mathrm{c.m.}},J) \sim \exp[-U(R_m,Z_1,A_1,J)/T_{max}(J)]$$

$$T_{max}(J) = \max\{T_{Z_1,A_1}(J)\}$$

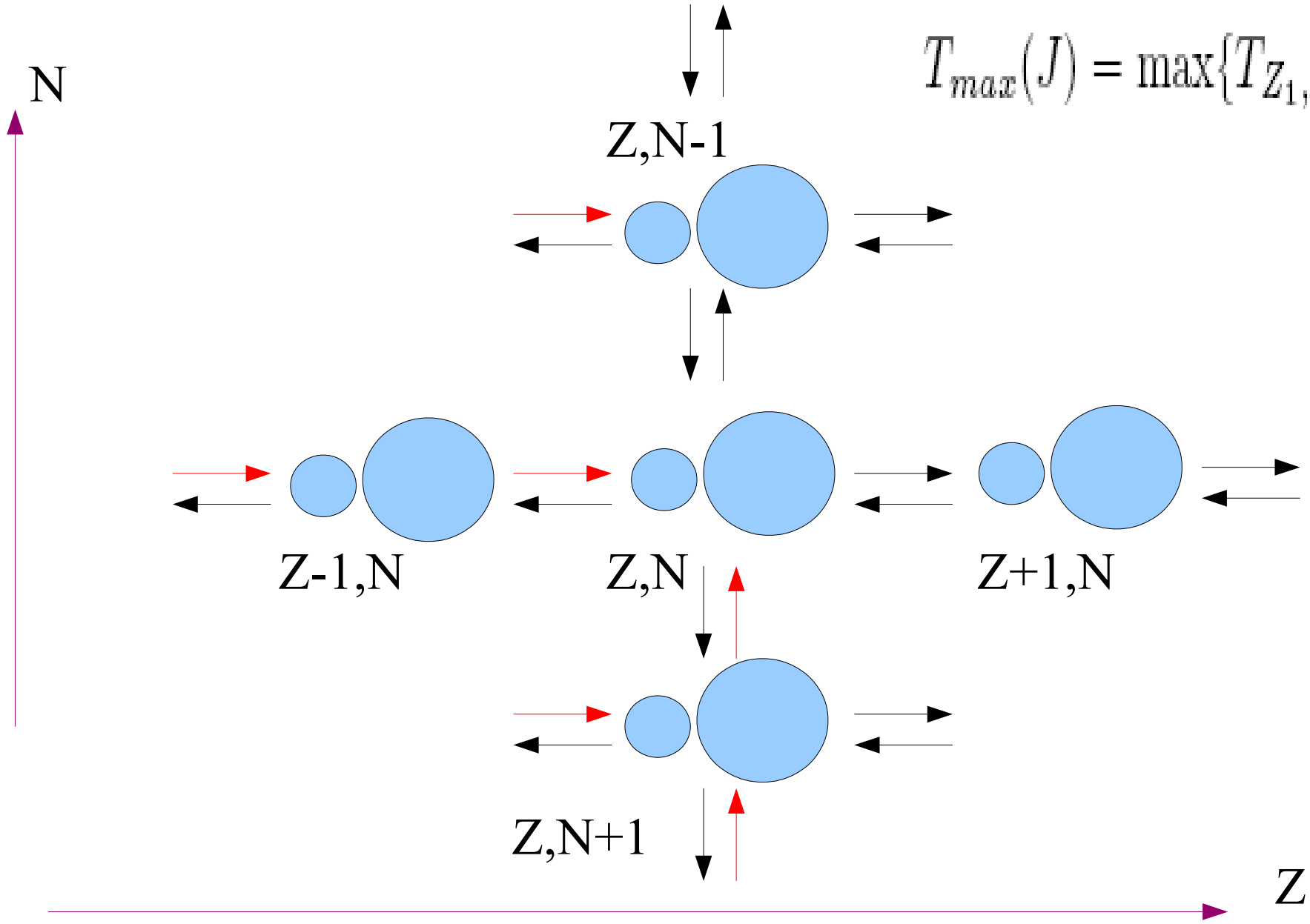

Potential energy of DNS

Driving potential:

$$U(R,Z,L)=B_1+B_2+V_N(R,Z,L)-B_{12}-V_{rot}^{CN}$$

$$V_N(R,Z,L)=V_{COUL}(R,Z)+V_{NN}(R,Z)+V_{rot}(R,L)$$

Nuclear potential we take as double folding potential:

$$V_{NN}(R,Z)=\int \rho_1(r_1)\rho_2(R-r_2)F(r_1-r_2)dr_1dr_2$$

Where nucleon-nucleon forces depend on nuclear densities:

$$F(r_1-r_2)=C_0(F_{in}\frac{\rho_0(r_1)}{\rho_0}+F_{ex}(1-\frac{\rho_0(r_1)}{\rho_0}))\delta(r_1-r_2)$$

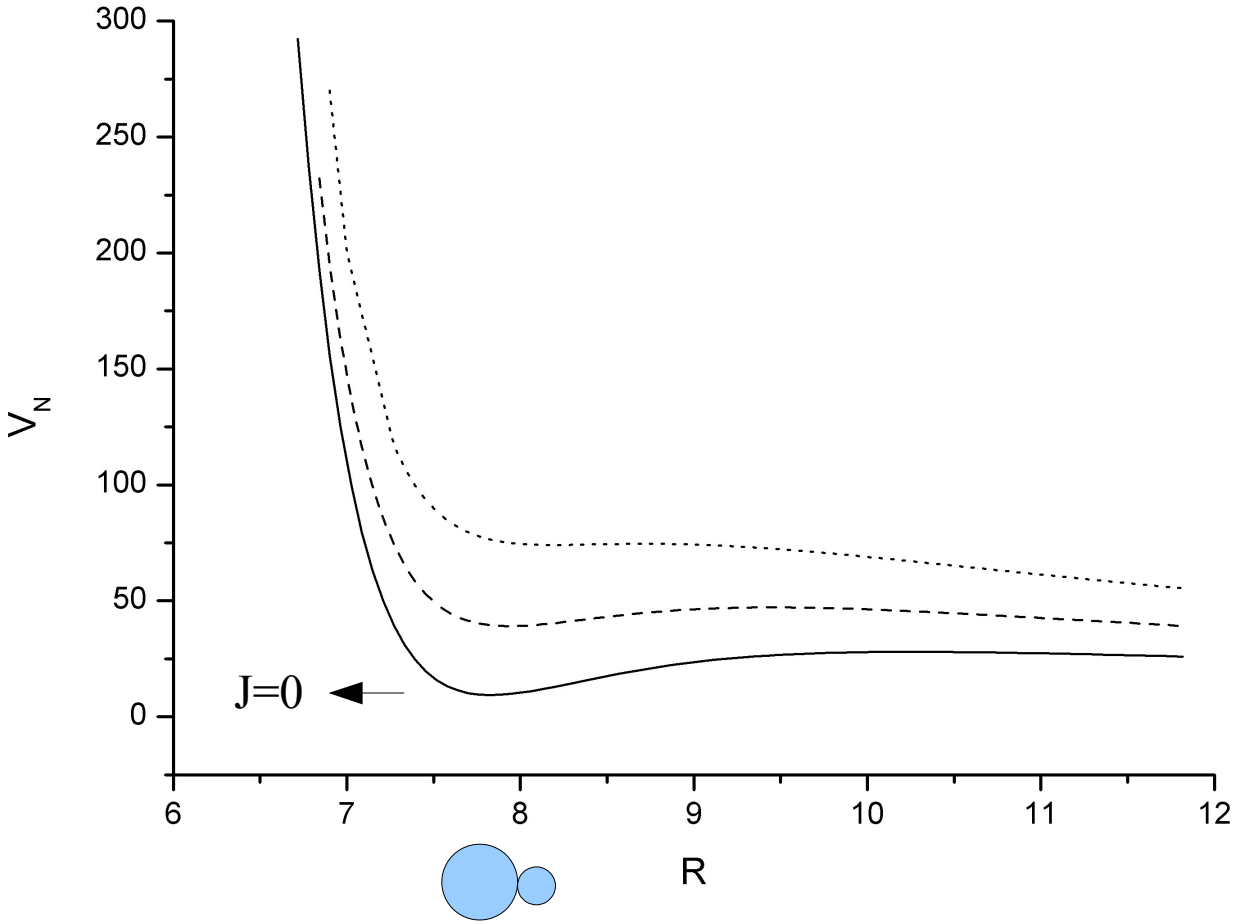

$R_{min}=R_1+R_2+0.5—1.5$ fm

$$P^{R}_{Z_1,A_1}(E_{\mathrm{c.m.}},J) \sim \exp[-B^{qf}_{R}(Z_1,A_1,J)/T_{Z_1,A_1}(J)]$$

The probability of the DNS decay in *R* coordinate

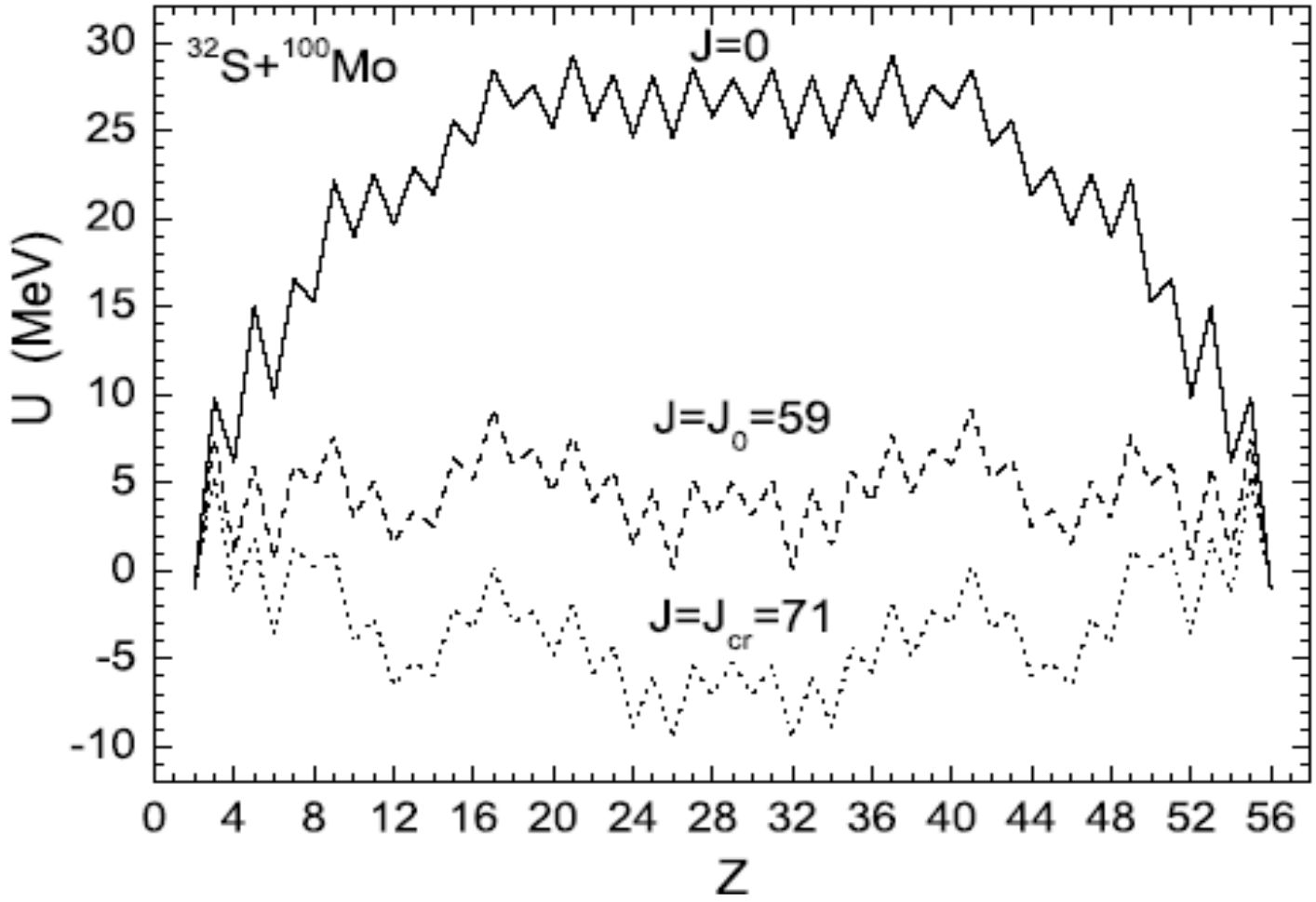

Driving potentials at different angular momenta J for the $^{32}\mathrm{S} + {}^{100}\mathrm{Mo}$ system. The value of U is normalized to the energy of the rotating CN. The value of A is related to Z to supply the minimum of U. The staggering of the lines reflects the odd-even effect.

At $J \geq J_0$ some DNS configurations become energetically favorable with respect to the CN configuration.

Table 1. The excitation energy E^*_{CN} of the CN at $J = 0$, the maximum kinematical angular momentum J^{kin}_{max}, the critical angular momentum J_{cr}, the angular momentum J_0, and the capture cross section σ_{cap} in the various reactions at incident energies indicated.

Reaction	$E_{\rm lab}$ MeV	E^*_{CN} MeV	J^{kin}_{max}	J_{cr}	J_0	σ_{cap} mb
^{32}S + ^{100}Mo	200	122	98	71	59	918
^{121}Sb + ^{27}Al	905	135	105	71	66	925
^{121}Sb + ^{27}Al	1030	157	118	71	66	813
^{40}Ar + ^{nat}Ag	247	128	118	82	63	857
^{40}Ar + ^{nat}Ag	337	193	160	82	63	628
^{40}Ar + ^{164}Dy	340	191	175	81	69	498

Then, normalized probabilities for any given decay channels are:

$$W_{Z,A}(E^*_{CN}, J) = \frac{P_{Z,A} P^R_{Z,A}}{\sum_{Z',A'} P_{Z',A'} P^R_{Z',A'}}$$

Cascade decay process of excited nuclear system is generated by Monte-Carlo method:

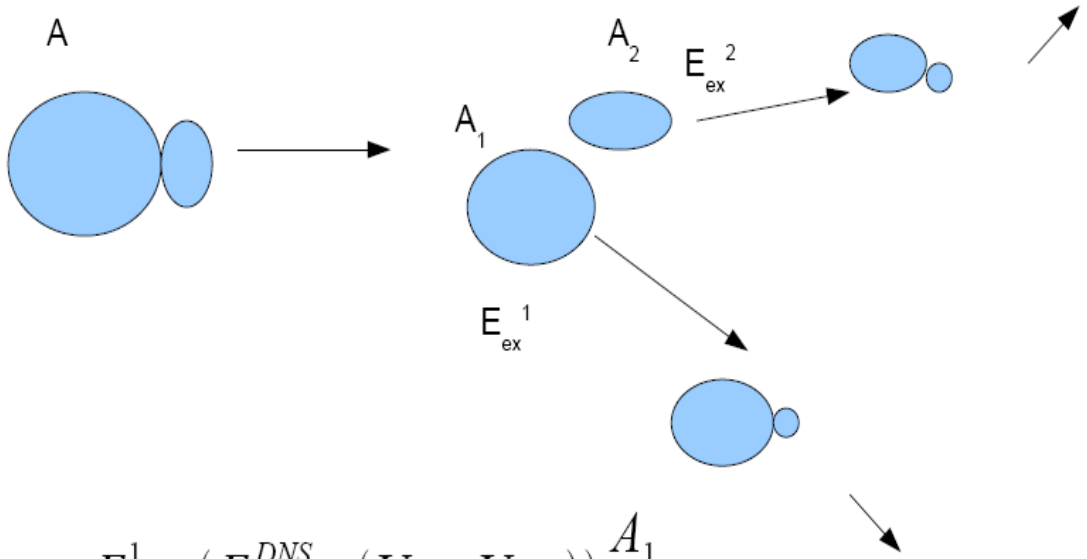

$$E^1_{ex} = (E^{DNS}_{ex} - (U_b - U_{min}))\frac{A_1}{A}$$

$$E^2_{ex} = (E^{DNS}_{ex} - (U_b - U_{min}))\frac{A_2}{A}$$

Nuclear temperature is determined as in Fermi-gas model as

$$T = \sqrt{(E^{ex}/a)} \qquad \textit{with} \qquad a = 0.1\tilde{1}4A + 0.162A^{2/3}$$

Particle multiplicities for a given *J*

$$M_i^{CN}(J) = N_i^{CN}(J)/N_{sim},$$

$$M_i^{FF}(J) = N_i^{FF}(J)/N_{sim},$$

where the number of emitted particles $N_i^{CN}(J)$ and $N_i^{FF}(J)$ $(i = n, p, d, t, {}^3\mathrm{He}, {}^4\mathrm{He})$ from the CN and from the fragments, respectively

N_{sim} is the number of simulations.

Total multiplicities are obtained by averaging over partial waves

$$M_i^k = \frac{\sum_{J=0}^{J_{max}} \sigma_{\mathrm{cap}}(E_{\mathrm{c.m.}}, J) M_i^k(J)}{\sum_{J=0}^{J_{max}} \sigma_{\mathrm{cap}}(E_{\mathrm{c.m.}}, J)},$$

Table 2. The calculated (theor.) and experimental (exp.) [2,3,6,17] production cross sections of the evaporation residues σ_{ER} and complex fragments σ_{FF}.

		Theor.		Exp.		
Reaction	$E_{\rm lab}$ MeV	σ_{ER} mb	σ_{FF} mb	σ_{ER} mb	σ_{FF} mb	Ref.
$^{32}S + ^{100}Mo$	200	700	218	828 ± 50	130 ± 13	[17]
$^{121}Sb + ^{27}Al$	905	605	320	752 ± 160	280 ± 60	[3]
$^{121}Sb + ^{27}Al$	1030	473	340	690 ± 130	395 ± 100	[3]
$^{40}Ar + ^{nat}Ag$	247	425	432	620 ± 80	550 ± 150	[6]
$^{40}Ar + ^{nat}Ag$	337	238	390	455 ± 50	520 ± 150	[6]
$^{40}Ar + ^{164}Dy$	340	33	465	31 ± 6	1194 ± 207	[2]

17. E. Vardaci *et al.*, Eur. Phys. J. A **43**, 127 (2010).

3. W.E. Parker *et al.*, Nucl. Phys. A **568**, 633 (1994).

6. R. Lacey *et al.*, Phys. Rev. C **37**, 2540 (1988).

2. D. Logan *et al.*, Phys. Rev. C **22**, 1080 (1980).

Results

Integrated evaporation residues, fusion-fission cross sections with corresponding alpha particle multiplicities

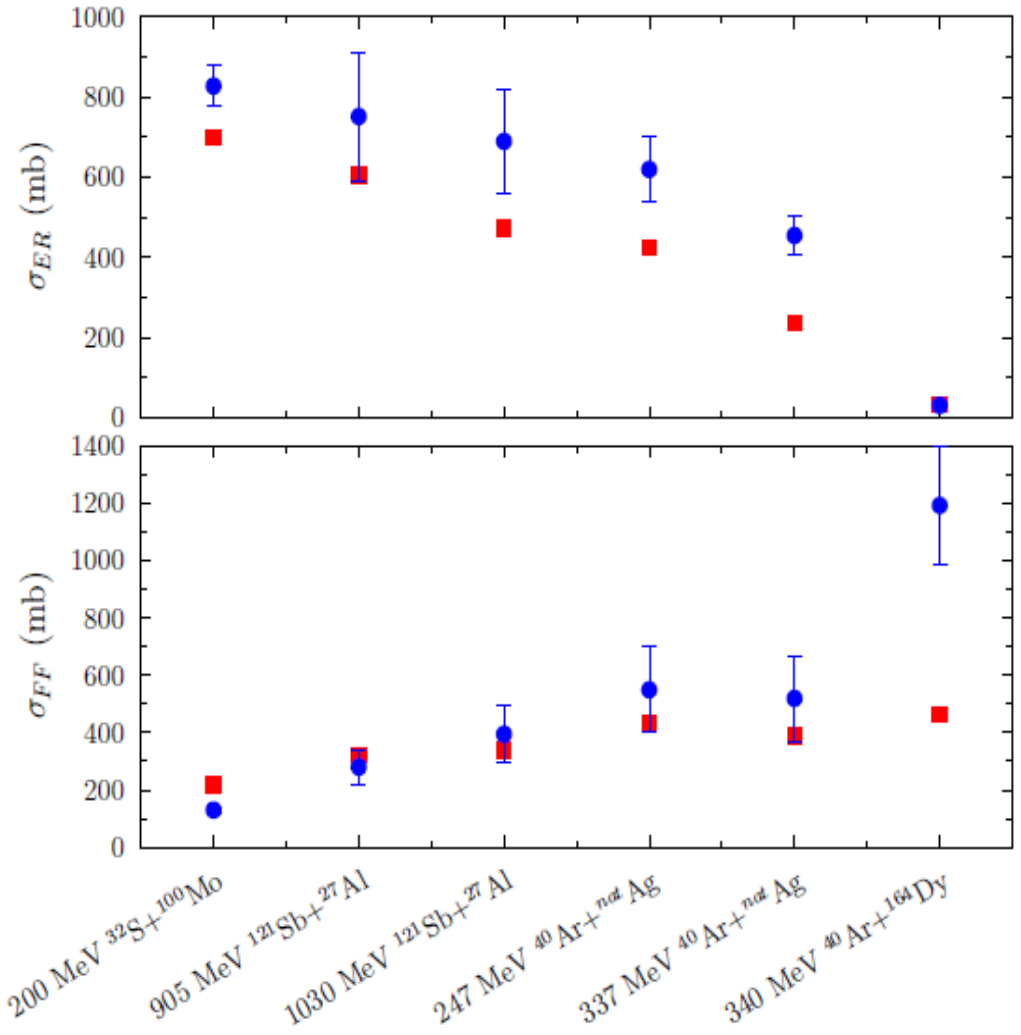

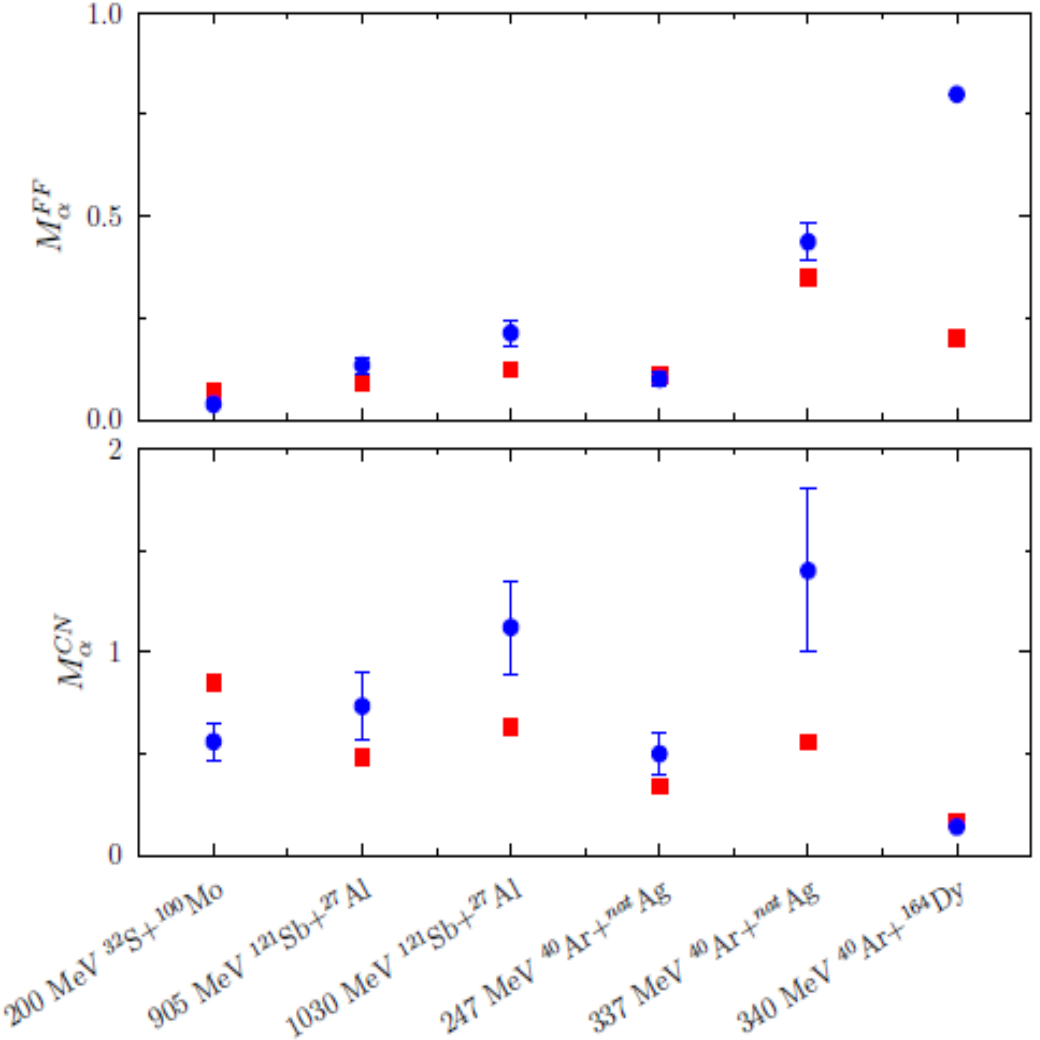

Proton multiplicities for a given reactions

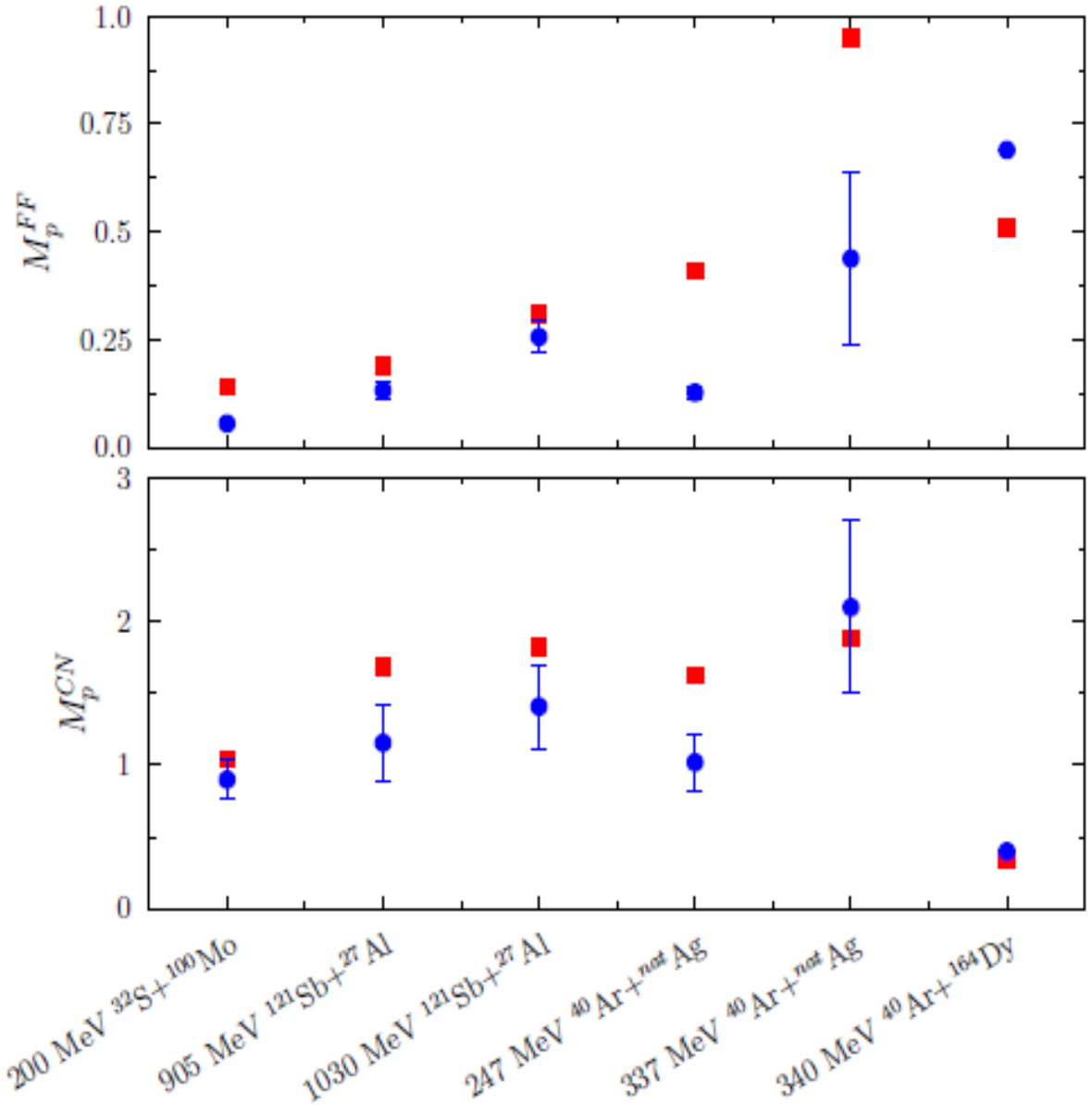

Table 3. Comparisons of the calculated (theor.) proton and α-particle multiplicities from the CN (M_p^{CN} and M_α^{CN}, respectively) and from the complex fragments (M_p^{FF} and M_α^{FF}, respectively) with experimental data (exp.) from refs. [2,3,6,17].

		Theor.		Theor.		Exp.		Exp.		
Reaction	$E_{\rm lab}$	M_p^{CN}	M_α^{CN}	M_p^{FF}	M_α^{FF}	M_p^{CN}	M_α^{CN}	M_p^{FF}	M_α^{FF}	Ref.
$^{32}S + ^{100}Mo$	200	1.04	0.85	0.14	0.068	0.9 ± 0.14	0.56 ± 0.09	0.055 ± 0.007	0.038 ± 0.005	[17]
$^{121}Sb + ^{27}Al$	905	1.69	0.48	0.19	0.09	1.156 ± 0.26	0.734 ± 0.17	0.132 ± 0.02	0.134 ± 0.02	[3]
$^{121}Sb + ^{27}Al$	1030	1.82	0.63	0.31	0.123	1.409 ± 0.29	1.122 ± 0.23	0.256 ± 0.038	0.213 ± 0.032	[3]
$^{40}Ar + ^{nat}Ag$	247	1.63	0.34	0.41	0.11	1.02 ± 0.2	0.5 ± 0.1	0.127 ± 0.015	0.1 ± 0.017	[6]
$^{40}Ar + ^{nat}Ag$	337	1.88	0.56	0.95	0.35	2.1 ± 0.6	1.4 ± 0.4	0.438 ± 0.2	0.437 ± 0.044	[6]
$^{40}Ar + ^{164}Dy$	340	0.34	0.17	0.51	0.2	0.4	0.14	0.69	0.8	[2]

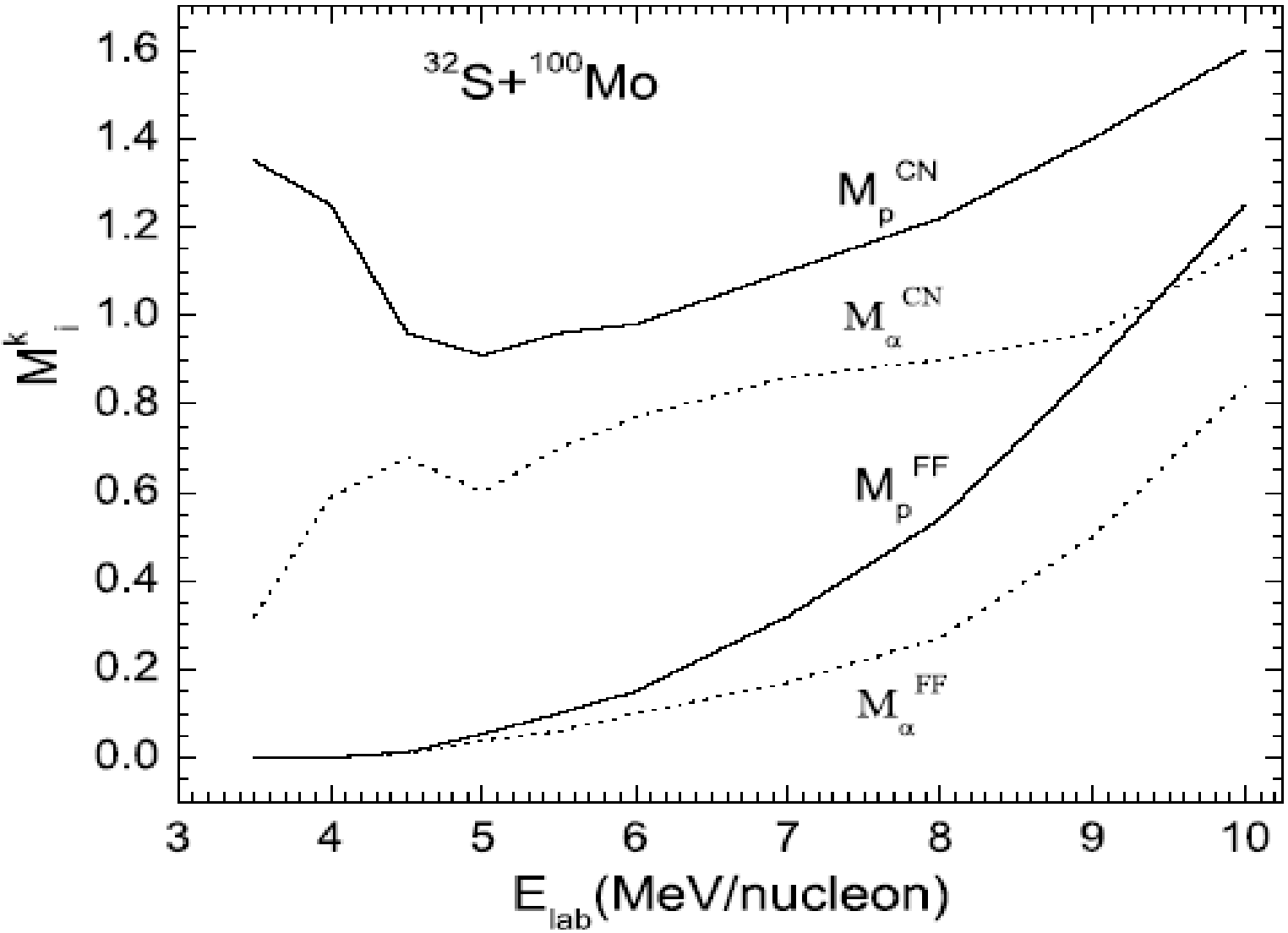

The calculated energy dependencies of proton (solid lines) and α-particle (dashed lines) multiplicities from the CN and from the complex fragments for the ^{32}S + ^{100}Mo reaction. Note that $J_{max} = J_0$ and $J_{max} = J_{cr}$ at $E_{\rm lab} =$ 4.3 and 4.9 MeV/nucleon, respectively.

From the comparison of the calculated LCP multiplicities and experimental data, we show the possible overlap of the decay products from different reaction mechanisms. With increasing the bombarding energy the ratio of the LCP multiplicity from the fission-like fragments to the LCP multiplicity from the CN increases due to the increase of fission and quasifission probabilities.

The simultaneous description of the LCP multiplicities and of the production cross sections of the evaporation residues and complex fragments gives us a chance to distinguish the reaction products from different reaction mechanisms.

The calculated LCP multiplicities show weak dependence on the reasonable variation of the level density parameter, and stronger dependence on the Coulomb barrier heights.

Synthesis of light *Xe* isotopes in complete fusion reactions via *xn* decay channels

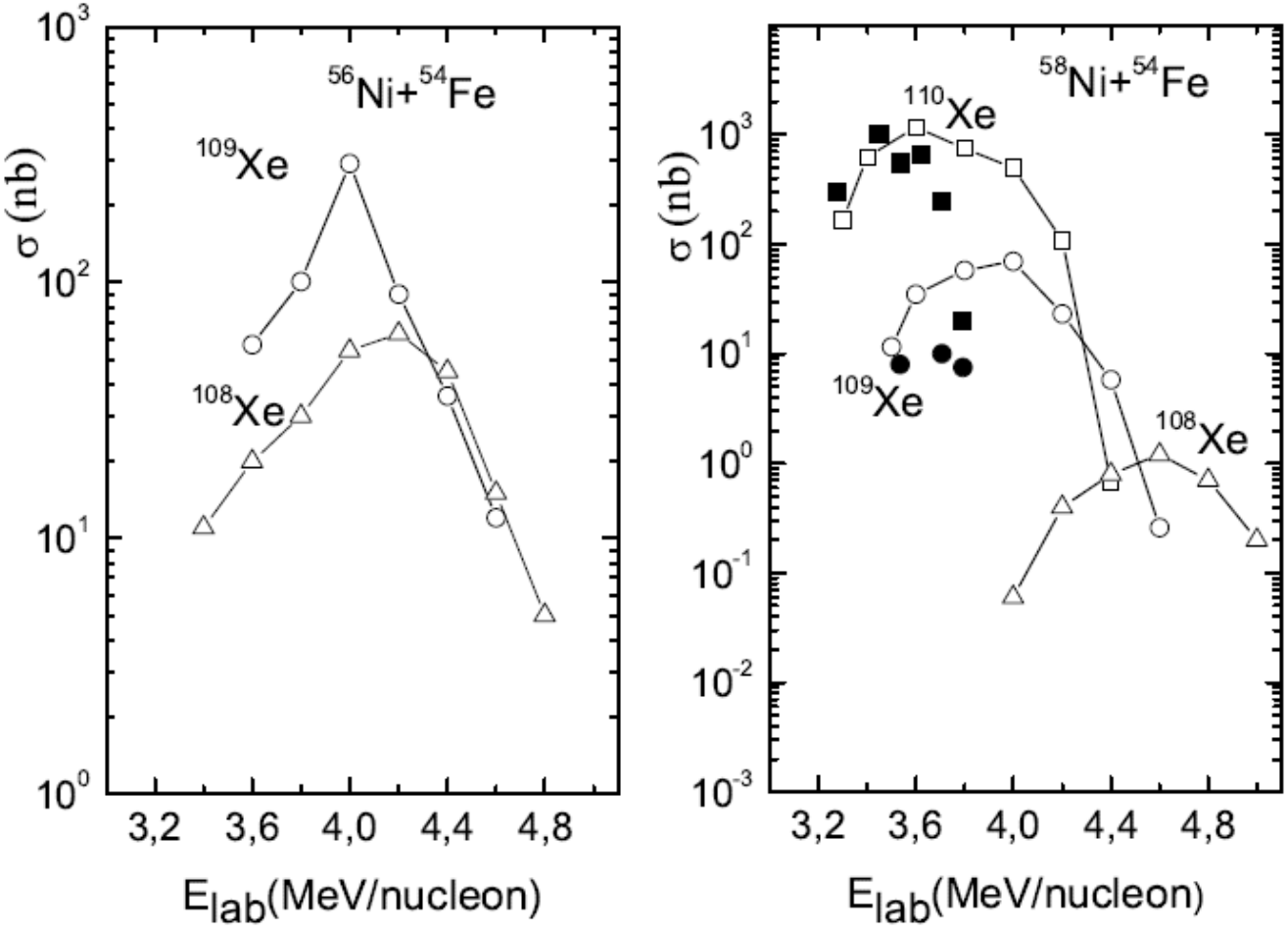

Sh. A. Kalandarov et al., Phys. Rev. C 93, 054607 (2016).

Synthesis of ^{100}Sn in complete fusion reaction via *xn* decay channel

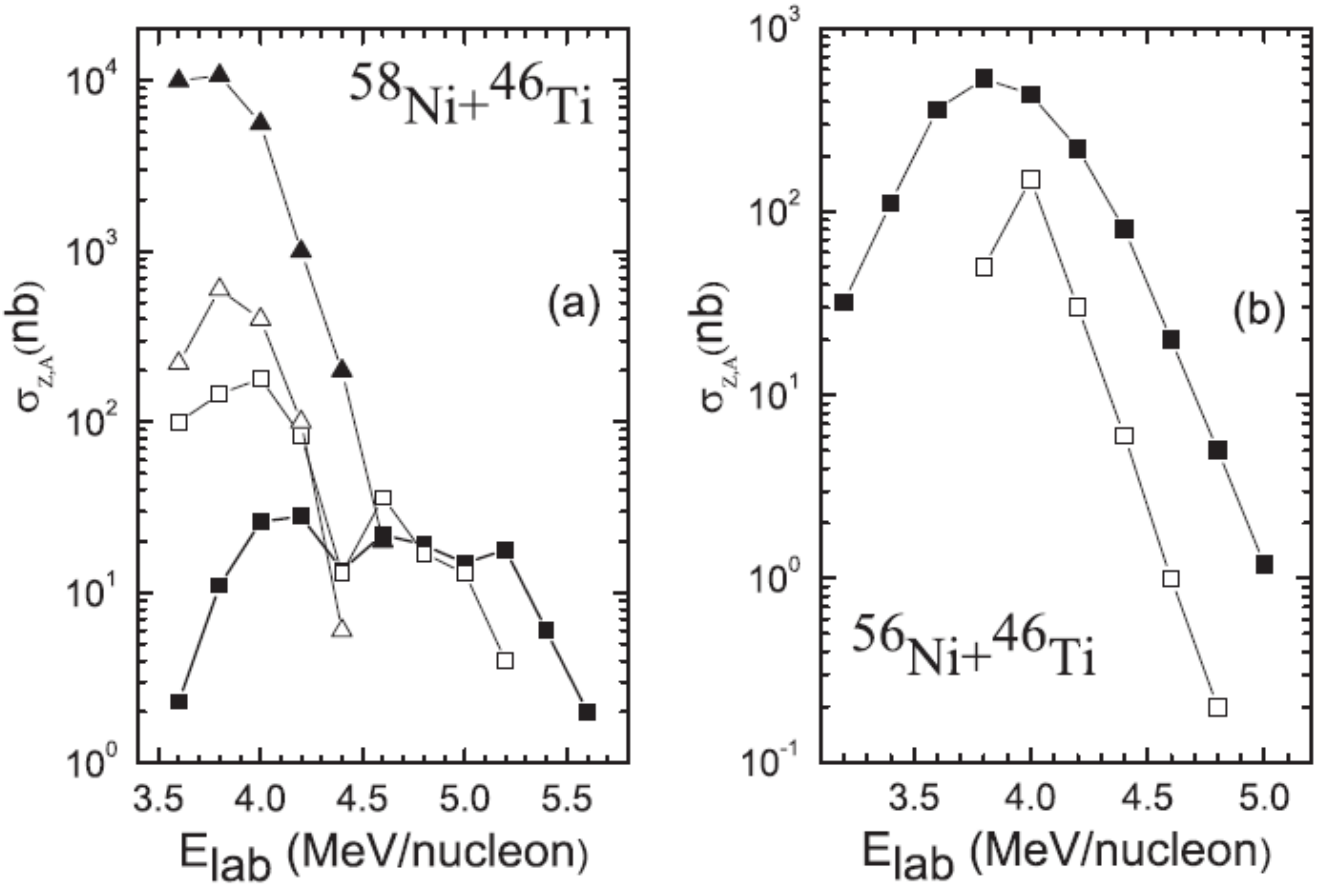

FIG. 2. The calculated excitation functions for the production of ^{100}Sn (■), ^{101}Sn (□), ^{102}Sn (▲), and ^{103}Sn (△) in *xn*-decay channels of the reactions (a) ^{58}Ni + ^{46}Ti and (b) ^{56}Ni + ^{46}Ti.

Sh. A. Kalandarov et al., Phys. Rev. C 90, 024609 (2014)

The model was applied to calculate the excitation functions for the production of neutron-deficient isotopes $^{108–110}$Xe and $^{112–114}$Ba in the fusion-evaporation reactions ^{56,58}Ni+^{54}Fe and ^{56,58}Ni+^{58}Ni with stable and radioactive beams.

The predicted maximum production cross sections of ^{108}Xe (^{112}Ba) are 63 nb (160 nb) and 1 nb (0.85 nb) in the reactions ^{56}Ni+^{54}Fe at 4.2 MeV/nucleon (4 MeV/nucleon) and ^{58}Ni+^{54}Fe at 4.6 MeV/nucleon (4.9 MeV/nucleon), respectively. In the reactions ^{56}Ni(4.4 MeV/nucleon)+^{58}Ni and ^{58}Ni(5.2 MeV/nucleon)+^{58}Ni, the production cross sections of ^{108}Xe are 23 nb and 0.32 nb, respectively.

Thus, using the ^{58}Ni+^{54}Fe reaction with a stable beam, one can study superallowed α-decay chains ^{108}Xe → ^{104}Te → ^{100}Sn and ^{112}Ba → ^{108}Xe → ^{104}Te → ^{100}Sn and the nuclear properties of the doubly magic nucleus ^{100}Sn with reasonable statistics.

Thank you for your attention

Summary

DNS model is applied to calculate the particle multiplicities in fusion-fission and quasifission reactions. The calculated particle multiplicities and integral cross sections are in good agreement with experimental data.

Calculations of energy and angular distributions of emitted light particles in different reaction channels are going on.

We also trying to take into account the preequilibrium emission and deep inelastic channel.